



Cite this: *Analyst*, 2016, **141**, 4204

## Sensing activity of cholinesterases through a luminescence response of the hexarhenium cluster complex $[\{\text{Re}_6\text{S}_8\}(\text{OH})_6]^{4-}$ †

Julia G. Elistratova,<sup>a</sup> Asiya R. Mustafina,<sup>\*a</sup> Konstantin A. Brylev,<sup>b</sup> Konstantin A. Petrov,<sup>a</sup> Michael A. Shestopalov,<sup>b</sup> Yuri V. Mironov,<sup>b</sup> Vasily M. Babaev,<sup>a</sup> Ildar K. Rizvanov,<sup>a</sup> Patrick Masson<sup>c</sup> and Oleg G. Sinyashin<sup>a</sup>

The present work describes a new method to sense cholinesterase-catalyzed hydrolysis of acetylcholine (ACh) through a luminescence response of the hexarhenium cluster complex  $[\{\text{Re}_6\text{S}_8\}(\text{OH})_6]^{4-}$ . A proton released from acetylcholinesterase (AChE)- or butyrylcholinesterase (BuChE)-catalyzed hydrolysis of ACh results in time-resolved sensitization of cluster-centered luminescence. The sensitization results from protonation of apical hydroxo-groups of the cluster complex. The protonation is affected by a counter ion effect. Thus, optimal conditions for adequate sensing of acetic acid produced by ACh hydrolysis are highlighted. Time-resolved luminescence and pH measurements under conditions of AChE-catalyzed hydrolysis of ACh show a good correlation between the cluster-centered luminescence and pH-induced inhibition of AChE. The inhibition is not significant within the first two minutes of ACh hydrolysis. Thus, the luminescence response measured within two minutes is dependent on both substrate and enzyme concentrations, which fits with AChE and BuChE kinetics. The usability of cluster-centered luminescence for monitoring the concentration-dependent inhibition of AChE with irreversible inhibitors is demonstrated, using a carbamylating agent, pyridostigmine bromide, as a model.

Received 10th March 2016,  
Accepted 31st March 2016

DOI: 10.1039/c6an00581k

www.rsc.org/analyst

## Introduction

Luminophores exhibiting metal-centered luminescence have gained increasing attention due to their unique photophysical properties, which minimize interference with biological background emissions. This makes such luminophores promising tools for biosensing.<sup>1–4</sup> In particular, luminescent hexanuclear cluster complexes of molybdenum and rhenium with the general formula  $[\{\text{M}_6(\mu_3\text{-X})_8\}\text{L}_6]^n$  (M = Mo and X = Cl, Br or I; M = Re and X = S or Se; L = apical organic or inorganic ligands) have gained great attention in the past decade due to their applicability as luminescent markers and X-ray contrast agents.<sup>5–13</sup> However, their analytical applicability is not well enough documented in the literature.<sup>2,14</sup> It is worth noting that the thermodynamic stability and/or kinetic inertness of the cluster core  $\{\text{M}_6(\mu_3\text{-X})_8\}$  along with the easy ligand

exchange of six apical ligands (L) are prerequisites for both low hazard and high tunability of cluster-centered luminescence.<sup>7–13,15–20</sup> Although the above-mentioned features of hexanuclear cluster complexes have a great impact on bio-sensing, no biosensing techniques based on cluster-centered luminescence have been reported so far. Sensing the activity of acetylcholinesterase (AChE) is of particular importance due to its crucial role in living systems in terminating the action of the neurotransmitter acetylcholine (ACh).<sup>21–24</sup> Moreover, inhibition of AChE by various chemicals is widely applied in the detection and monitoring of carbamates and organophosphorus pesticides and chemical warfare nerve agents<sup>25–27</sup> and in the development of cholinesterase inhibitors for palliative treatment of Alzheimer's disease and *myasthenia gravis*.<sup>28–31</sup> Numerous techniques have been reported for determination of cholinesterase (ChE) activity and its inhibition. Colorimetric, spectrophotometric, fluorometric, radiometric, electrochemical and potentiometric techniques have been applied to measure the acetic acid or choline produced by enzymatic hydrolysis of acetylcholine.<sup>22–24</sup> Taking into account pH-induced inhibition of AChE,<sup>32,33</sup> measurements in buffer solutions are more widely applied in sensing enzymatic activity than determination of the released acetic acid in pH-variant media. The popular Ellman method measures AChE activity

<sup>a</sup>A. E. Arbuzov Institute of Organic and Physical Chemistry, Kazan Scientific Center, Russian Academy of Sciences, 8 Arbuzov str., 420088 Kazan, Russian Federation.  
E-mail: asiyaust@mail.ru

<sup>b</sup>Nikolaev Institute of Inorganic Chemistry SB RAS, 3 Acad. Lavrentiev Ave., 630090 Novosibirsk, Russian Federation

<sup>c</sup>Kazan Federal University, 18 Kremlyovskaya str., 420008 Kazan, Russian Federation

† Electronic supplementary information (ESI) available. See DOI: 10.1039/c6an00581k



under pH invariant buffer conditions.<sup>34</sup> Its wide use arises from its simplicity, accuracy and low cost. Moreover, it is easily adaptable for automated analyzers or plate readers for rapid processing of large numbers of samples.<sup>24,35</sup> However, interference of the chromogene 5-thio-2-nitrobenzoic acid absorption with the Soret band of hemoglobin restricts applicability of the method to whole blood samples.<sup>36</sup> In addition, the substrate analogue used in Ellman's method, acetyl/butrylthiocholine, interferes with certain chemicals, in particular oximes, the ChE reactivators used in the treatment of organophosphate poisoning. The use of indoxylacetate instead of acetylthiocholine is an alternative procedure for sensing inhibition of AChE activity.<sup>37</sup> However, indoxylacetate is also hydrolyzed by lipases and carboxylesterases. Recently published articles devoted to fluorescent detection of AChE activity<sup>38–42</sup> are based on the use of thio-esters instead of ACh. Thus, development of new techniques to sense cholinesterase activity through monitoring ACh hydrolysis is still of great interest.

Our recent work reported a nanotechnology-based fluorescent technique based on the H-function of Tb(III) complexes included in silica nanoparticles.<sup>43</sup> The results highlighted the main requirements for the H-function sensor for accurate and adequate determination of AChE activity. The first requirement is high sensitivity, because pH-induced spectral changes have to be monitored within the first few minutes of enzyme hydrolysis before inhibition of AChE due to pH lowering. The second requirement is a retarded ion exchange, preventing metal ion-induced inhibition of AChE.<sup>44–46</sup> Thus, anionic complexes with slow ion exchange and sensitive H-function are applicable in sensing enzymatic hydrolysis of ACh.

The hexarhenium cluster complex  $[\{\text{Re}_6\text{S}_8\}(\text{OH})_6]^{4-}$  (Scheme 1), where a  $\text{Re}_6$  octahedron is strongly bonded with eight inner  $\mu_3\text{-S}$  ligands into the cluster core  $\{\text{Re}_6\text{S}_8\}^{2+}$ , while the six apical hydroxo ligands are protonable, fits the above-mentioned requirements for the H-sensor.<sup>47</sup> The specific structure of  $[\{\text{Re}_6\text{S}_8\}(\text{OH})_6]^{4-}$  determines  $\text{H}^+$ -induced stepwise protonation of apical  $\text{OH}^-$  ligands (equilibria (1) and (2)) with subsequent changes in cluster-centered photoluminescence.<sup>47</sup>

The present work deals with the luminescence response of  $[\{\text{Re}_6\text{S}_8\}(\text{OH})_6]^{4-}$  upon medium acidification resulting from the enzymatic hydrolysis of ACh as the basis for sensing. The work

shows that time-resolved luminescence measurements at various enzyme and substrate concentrations follow the kinetics of both AChE- and BChE-catalyzed hydrolysis of ACh.<sup>48,49</sup> Moreover, the applicability of cluster-centered luminescence in sensing cholinesterase inhibitors is reported. The inhibition effect is exemplified by using the drug pyridostigmine bromide (PyrBr) as a model inhibitor.<sup>27,50,51</sup>

## Experimental

### Materials and synthesis

Choline chloride (99% purity), acetylcholine chloride ( $\geq 99\%$  purity), pyridostigmine bromide, acetylcholinesterase (AChE) from *Electrophorus electricus* (electric eel, Type VI-S, lyophilized powder, 200–1000 units per mg protein) were purchased from Sigma-Aldrich (Saint Louis, USA). Human butyrylcholinesterase (BuChE) was highly purified from human plasma as described.<sup>52</sup>  $\text{K}_4[\{\text{Re}_6\text{S}_8\}(\text{OH})_6]\cdot 8\text{H}_2\text{O}$  was synthesized and purified according to a previously published procedure.<sup>53</sup>

**Sample preparation for luminescence detection of ACh hydrolysis.** A stock solution of AChE ( $C = 10^{-6}$  M) was prepared by vortex-assisted dissolution of the lyophilized enzyme in NaCl (100 mM). Stock solution of BuChE  $6.7 \times 10^{-7}$  M was prepared in 50 mM phosphate buffer pH 8.0. The solutions were stored at 8 °C for no more than 2–3 days before use.

The mixture of  $\text{K}_4[\{\text{Re}_6\text{S}_8\}(\text{OH})_6]\cdot 8\text{H}_2\text{O}$  (0.0075 mM), NaCl (1 mM) and AChE (pH 8.4) was incubated for 5 minutes at 25 °C. Then ACh was added, and its hydrolysis immediately monitored through cluster-centered luminescence. The AChE concentration was varied in the range  $10^{-9}$ – $2 \times 10^{-8}$  M. The ACh concentration was varied from 0.06 to 0.9 mM. The luminescence spectrum kinetics was recorded at 25 °C every minute within 10 min.

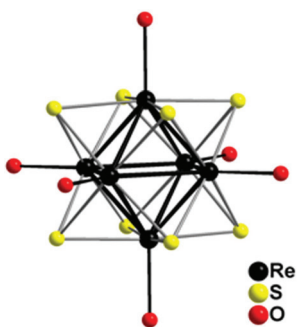
## Methods

Steady-state uncorrected emission spectra were recorded on a fluorescence spectrophotometer Cary Eclipse (Agilent Technologies) under aerated conditions. Excitation was at  $\lambda = 350$  nm, and emission was detected at 600–650 nm, excitation and emission slits were 10 nm.

pH of solutions was controlled with a Microprocessor pH meter "pH 212" (Hanna Instruments). The pH-meter was calibrated with standard aqueous buffer solutions.

ESI measurements were performed on an AmazonX (Bruker Daltonics, Germany) mass spectrometer in the negative mode. Nitrogen (15 psi) was used for desolvation and nebulization. The sample introduction rate was  $0.2 \text{ mL min}^{-1}$ . The ESI source conditions were as follows: capillary voltage 4500 V, capillary exit voltage  $-140$  V, dry gas temperature 300 °C. Mass spectra were acquired at an  $m/z$  range from 100 to 2000.

All samples were prepared in bi-distilled water filtered through a  $0.45 \mu\text{m}$  Millipore nylon membrane filter. All measurements were performed at least in triplicate at 25 °C. The standard deviation of each point was about 2–3%.



**Scheme 1** Structure of the cluster complex  $[\{\text{Re}_6\text{S}_8\}(\text{OH})_6]^{4-}$ . Hydrogen atoms are not shown.



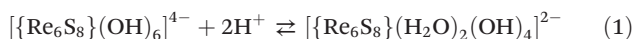
## Results and discussion

### Acidification effect on the cluster-centered luminescence in acetic acid solution

The response ability of the cluster-centered luminescence to acidification in acetic acid solutions is a prerequisite in developing a new sensing technique for enzymatic hydrolysis of acetylcholine. Indeed, the amount of acetic acid (or protons) produced measures the rate of ACh hydrolysis, *i.e.* the enzyme activity:  $d[H^+]/dt = -d[ACh]/dt$ .

As previously reported, dissolution of  $K_4\{Re_6S_8\}(OH)_6 \cdot 8H_2O$  in water is followed by turning the anionic complex  $[\{Re_6S_8\}(OH)_6]^{4-}$  to  $[\{Re_6S_8\}(H_2O)_2(OH)_4]^{2-}$  through equilibrium (1).<sup>47</sup> The self-maintained pH of aqueous  $K_4\{Re_6S_8\}(OH)_6 \cdot 8H_2O$  solution is 8.4. Its luminescence is manifested by a broad and structureless emission band with a maximum wavelength around 625 nm according to the spectrum recorded within the current study by the fluorescence spectrophotometer Cary Eclipse. It is well known that the phosphorescence of hexarhenium cluster complexes in solutions is somewhat quenched by oxygen. Thus, deaeration by purging an inert gas stream is commonly used for determination of correct emission quantum yield and lifetime values for hexarhenium clusters in solutions. Nevertheless, the presented luminescence measurements were carried out without deaeration, since it is a time-consuming process, which restricts revealing the quick response of the cluster luminescence on the acid produced by AChE-catalyzed ACh hydrolysis. Moreover, performing time resolved emission measurements in an aerated solution retains the oxygen effect on the cluster emission at a similar level without a disturbance of the emission intensity caused by a gradual change of oxygen concentration.

ESI mass spectrometry was performed in order to detect  $[\{Re_6S_8\}(H_2O)_2(OH)_4]^{2-}$  in solution. The ESI spectrum (Fig. 1) confirms predominance of the cluster di-anion in aqueous solution of  $K_4\{Re_6S_8\}(OH)_6 \cdot 8H_2O$  at pH 8.4.



Thus, equilibrium (2) is the fundamental principle for sensing proton release through cluster-centered luminescence. Fig. 2a shows the enhancement of emission intensity upon

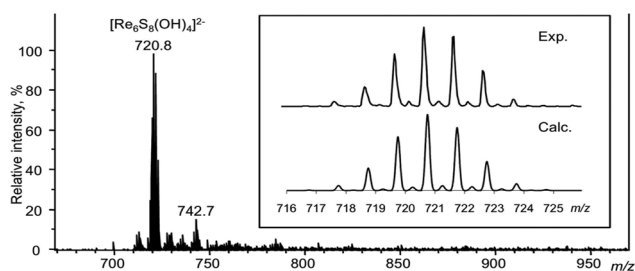


Fig. 1 ESI mass spectrum of an aqueous solution of  $K_4\{Re_6S_8\}(OH)_6 \cdot 8H_2O$  (0.0075 mM, pH = 8.4).

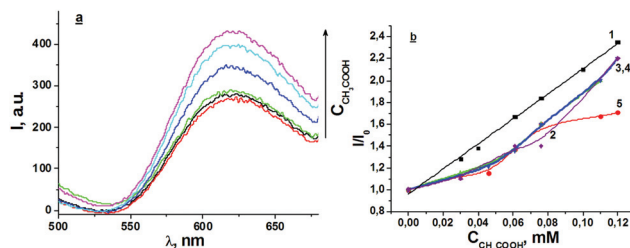


Fig. 2 (a) Emission spectra of the cluster complex (0.0075 mM) in acetic acid solutions ( $\lambda_{ex} = 350$  nm). Arrow designates the tendency with increased concentration in acetic acid from 0 to 0.1 mM. (b)  $I/I_0$  ratio for the aqueous solution of  $K_4\{Re_6S_8\}(OH)_6 \cdot 8H_2O$  (0.0075 mM) in the presence of different concentrations of acetic acid without any additives (1) and in the presence of various additives: 0.075 mM ChCl (2), 0.075 mM ACh (3),  $10^{-8}$  M AChE and 1 mM NaCl (4), 0.1 M NaCl (5).

addition of acetic acid to the aqueous solution of  $K_4\{Re_6S_8\}(OH)_6 \cdot 8H_2O$ . This is quantitatively represented by  $I/I_0$  values in Fig. 2b, where  $I$  and  $I_0$  are emission intensities at 625 nm in solutions of acetic acid and solutions without additives (at pH 8.4), respectively. Although  $[\{Re_6S_8\}(H_2O)_2(OH)_4]^{2-}$  should be predominant at pH 8.4, some minor contributions of  $[\{Re_6S_8\}(OH)_6]^{4-}$  equilibrated with the latter cannot be ruled out. The experimentally observed increase in  $I/I_0$  (Fig. 2b) confirms that protonation of  $[\{Re_6S_8\}(H_2O)_2(OH)_4]^{2-}$  according to equilibrium (2) is the cause for the observed trend. The increase is linear up to 0.12 mM acetic acid. Beyond this concentration, precipitation occurs. This fact confirms the formation of a poorly water-soluble neutral complex  $[\{Re_6S_8\}(H_2O)_4(OH)_2]$  according to equilibrium (2). Thus, linear increase in  $I/I_0$  with acetic acid concentration up to 0.12 mM is the prerequisite for the H-function of the cluster complex under these concentration conditions.

The equilibria between differently charged clusters can be shifted by interactions with counter-ions released by inorganic or biological components in the medium. Moreover, a possible apical hydroxide ligand substitution to enzyme donor groups or any anions from inorganic and/or biological background may be another cause for the background effect on the H-function of the cluster. Thus, monitoring the enzymatic hydrolysis through cluster-centered luminescence should be preceded by evaluation of the effects of inorganic, organic and biological background on the luminescence response in acetic acid solutions. For this reason,  $I/I_0$  values were determined in acetic acid solutions following addition of ChCl, ACh and AChE in NaCl (1 mM) solution.  $I/I_0$  was increased with acetic acid concentration, although the increase was affected by the presence of ACh, ChCl and AChE (plots 2–4 in Fig. 2b). In particular, the increase becomes less pronounced in the acetic acid concentration range 0–0.05 mM, while more enhanced and close to linear increase in  $I/I_0$  is observed at 0.05–0.125 mM (curves 2–4 in Fig. 2b). A shift of equilibria (1) and (2) towards cluster anions  $[\{Re_6S_8\}(OH)_6]^{4-}$  and  $[\{Re_6S_8\}(H_2O)_2(OH)_4]^{2-}$ , respectively resulted from ion-pairing of the anions with both organic and inorganic cations. This ion-pairing is one of the reasons



for the background effect. Nevertheless, no specific influence of AChE on both luminescence and the H-function of the cluster was detected. The background effect on the H-function of the cluster becomes enhanced in more concentrated (0.1 M) NaCl solutions. The concentration profile of  $I/I_0$  at 0.1 M NaCl lies below curves 1–4. This indicates the restricted H-function of the cluster under these conditions.

Thus, NaCl concentration was maintained at 1 mM in all measurements to avoid the undesirable counter-ion effects.

### Time-resolved luminescence measurements of the cluster complex solution under conditions of AChE-catalysed ACh hydrolysis

As above-mentioned, the concentration of acetic acid produced by AChE-catalysed ACh hydrolysis is affected by pH-induced inhibition of the enzyme.<sup>32,33</sup> The optimum of AChE activity is at pH 8. Activity decreases with acidification because of protonation of the catalytic triad histidine. Thus, time-resolved pH measurements during AChE-catalysed ACh hydrolysis in the presence of the cluster complex were performed. They are represented in Fig. 3 by curve 1. Results indicate that pH drops from 8.4 to 7.0 within four minutes of hydrolysis.

Curve 2 in Fig. 3 shows the change in cluster-centered luminescence intensity ( $I/I_0$  values) with time under enzymatic hydrolysis of ACh.

The change in  $I/I_0$  versus time, *i.e.*, change versus the actual pH, is sigmoidal with the inflexion point after 3 minutes of hydrolysis (curve 2 in Fig. 3). This results from time-dependent acidification (curve 1 in Fig. 3) with subsequent inhibition of AChE. A comparison of curves 1 and 2 indicates that the inflexion point is around pH 7.2, which corresponds to protonation of a key group in AChE, *i.e.*, the catalytic triad histidine.<sup>48</sup> The increase in  $I/I_0$  within first 3 minutes (curve 1 in Fig. 3) is similar to the trend shown in Fig. 2b: dependence of  $I/I_0$  on acetic acid concentration. This confirms that the  $I/I_0$  values arise from enzymatic hydrolysis of ACh (Fig. 3). Moreover, these values follow the time-dependent pH-induced inhibition of enzymatic activity. This fact raises a question about correlation between  $I/I_0$  determined within the first minutes of ACh hydrolysis with the enzymatic hydrolysis rate.

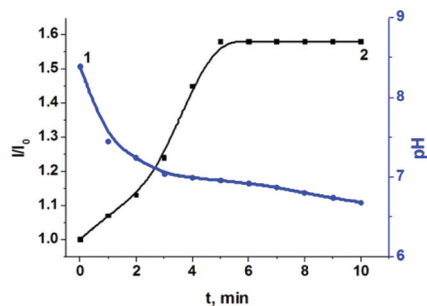


**Fig. 3** Time dependencies of pH (1) and  $I/I_0$  (2) in solution of the cluster complex (0.0075 mM),  $2 \times 10^{-8}$  M AChE, 1 mM NaCl. The enzymatic hydrolysis started by adding 0.4 mM ACh at  $t = 0$ .

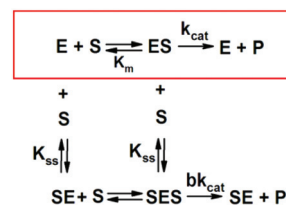
### Enzyme and substrate effects on time-resolved luminescence measurements of the cluster complex solution

Scheme 2 describes AChE ( $E$ )-catalyzed hydrolysis of ACh. The hydrolysis kinetics at low substrate ( $S$ ) concentration corresponds to the boxed reactions in Scheme 2. The hydrolysis rate increases with ACh concentration up to 0.5 mM,<sup>48,49</sup> which corresponds to Michaelis–Menten kinetics, *i.e.*  $b = 1$  in eqn (3). Substrate-induced inhibition of AChE is observed at greater ACh concentration, which corresponds to  $b < 1$  in eqn (3). Time-resolved  $I/I_0$  measured at various substrate concentrations under constant AChE concentration are presented in Fig. 4a. Fig. 4b shows the values determined within two minutes of hydrolysis versus ACh concentration. It is worth noting that experimentally observed changes in  $I/I_0$  measured within two minutes upon increase of ACh concentration are greater than the standard deviation of  $I/I_0$  values. Dependence of  $I/I_0$  on ACh concentration is represented by two sets of experimental points (curves 1 and 2 in Fig. 4b) in order to show the reproducibility of  $I/I_0$  values. Similarity of the determined values confirms the reliability of the revealed tendency.

$$v = \frac{k_{\text{cat}}[E]}{1 + K_m/[S]} \left( \frac{1 + b[S]/K_{\text{SS}}}{1 + [S]/K_{\text{SS}}} \right). \quad (3)$$

where  $k_{\text{cat}}$  is the catalytic constant,  $[E]$  the enzyme concentration, and  $K_m$  the Michaelis–Menten constant. The  $b$  factor refers to the effect on the  $k_{\text{cat}}$  of a second  $S$  molecule that binds to  $E$  to form SES with a dissociation constant  $K_{\text{SS}}$ .<sup>48</sup>

The profile of observed dependence (Fig. 4b) reveals the increase of  $I/I_0$  up to 0.5 mM ACh, followed by the decrease at



**Scheme 2** Schematic mechanism of cholinesterase ( $E$ )-catalyzed hydrolysis of positively charged substrates ( $S$ ), the factor  $b$  reflects the efficiency of product formation from the ternary complex SES.<sup>48</sup>

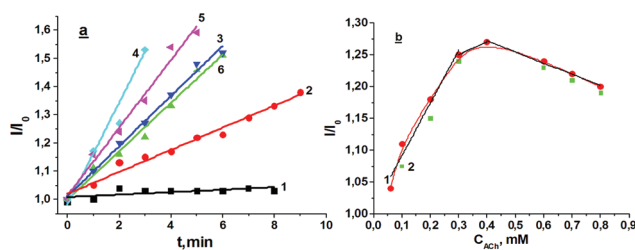


**Fig. 4** (a)  $I/I_0$  versus time measured in solutions of the cluster complex (0.0075 mM),  $2 \times 10^{-8}$  M AChE, 1 mM NaCl at various concentrations of ACh: 0.06 mM (1), 0.1 mM (2), 0.2 mM (3), 0.4 mM (4), 0.6 mM (5), 0.8 mM (6). (b)  $I/I_0$  values determined after two minutes of hydrolysis versus ACh concentration at  $2 \times 10^{-8}$  M AChE, 1 mM NaCl (1, 2).



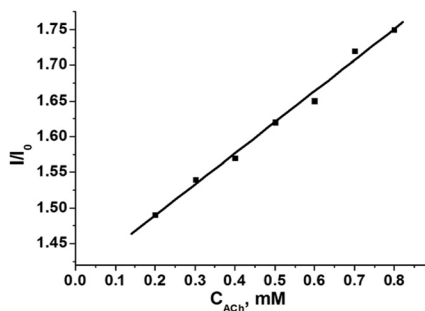


Fig. 5  $I/I_0$  determined after two minutes of ACh hydrolysis for the cluster complex solution (0.0075 mM),  $2 \times 10^{-8}$  M BuChE and different concentrations of ACh.

ACh concentration above 0.5 mM. This is in agreement with the above-mentioned substrate-induced activation with  $b = 1$  and inhibition with the  $b < 1$  kinetic model (eqn (3), Scheme 2).<sup>48</sup>

The enzymatic hydrolysis rate of ACh is greatly affected by the enzyme nature or structure. For example, no substrate-induced inhibition is observed for BuChE-catalyzed hydrolysis of ACh within the concentration range 0.2–0.9 mM according to the kinetics of BuChE-catalyzed hydrolysis of ACh.<sup>33</sup> Instead, BuChE shows activation by excess substrate. The corresponding dependence of the hydrolysis rate on substrate concentration is described by eqn (3) with  $b > 1$ . Thus, similar luminescence measurements at various ACh concentrations were performed for BuChE. The time dependencies of  $I/I_0$  are available in the ESI (Fig. S1†). The linear increase in  $I/I_0$  as a function of ACh concentrations up to 0.8 mM (Fig. 5) is also in agreement with the kinetics of BuChE-catalyzed hydrolysis of ACh.<sup>33</sup>

The effect of enzyme concentration on  $I/I_0$  was exemplified by luminescence measurements at different AChE concentrations.  $I/I_0$  for 0.4 mM ACh versus AChE concentration is represented in Fig. 6, while the corresponding time-resolved measurements are presented in the ESI (Fig. S2†). It is worth noting that  $I/I_0$  values measured at 0.1 mM ACh exhibit similar dependence on AChE concentration (Fig. S3 in the ESI†).

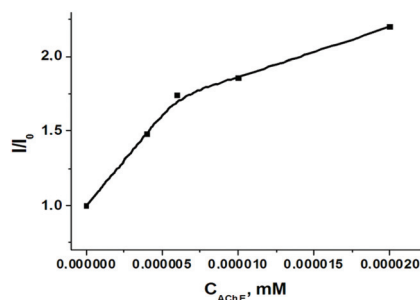


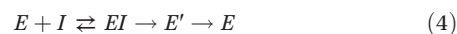
Fig. 6  $I/I_0$  measured after two minutes in the cluster complex solution (0.0075 mM), 0.4 mM ACh, 1 mM NaCl and different concentrations of AChE.

According to enzyme kinetics theory, the rate of AChE-catalyzed hydrolysis of ACh should exhibit a linear dependence on enzyme concentration.<sup>48,49</sup> The plot of  $I/I_0$  versus AChE concentration is curvilinear (Fig. 6). Taking into account that  $I/I_0$  values are affected by proton-induced transformation of  $[\{\text{Re}_6\text{S}_8\}(\text{H}_2\text{O})_2(\text{OH})_4]^{2-}$  to  $[\{\text{Re}_6\text{S}_8\}(\text{H}_2\text{O})_4(\text{OH})_2]$  through equilibrium (2), the observed deviation suggests that this transformation is affected by AChE above a certain concentration of the enzyme. This tendency may result from the buffer effect of AChE, which possesses numerous basic groups (His, Lys, Arg) on the solvent-exposed surface and/or the decreased equilibrium concentration of the cluster complexes due to their interactions with the enzyme.

Thus, the results highlight the correlation between the cluster-centered luminescence and activity of AChE. It is worth noting once more that certain drugs, including the carbamylating agent pyridostigmine bromide, inhibit AChE activity.<sup>50,51</sup> This raises a question about the detection of inhibitory action through cluster-centered luminescence.

#### Inhibition of AChE by pyridostigmine bromide as monitored by luminescence

Inhibition reaction of AChE by pyridostigmine bromide (PyrBr, I) can be described by the following two-step mechanism (4).<sup>32</sup>



The quick reversible complex formation ( $EI$ ) is followed by carbamylation of the enzyme active serine ( $E'$ ) with a reaction rate constant  $k_2$ . The inhibition is quasi-irreversible, since slow water-mediated decarbamylation of  $E'$  occurs with a reaction rate constant  $k_3$ , resulting in enzyme regeneration.<sup>50,54</sup> Enzyme reactivation is slow enough to be insignificant within the experimental time frame conditions. Thus, under our experimental conditions, inhibition may be considered as irreversible.

Fig. 7 illustrates time dependencies of  $I/I_0$  for AChE-catalyzed hydrolysis of ACh in the presence of different PyrBr

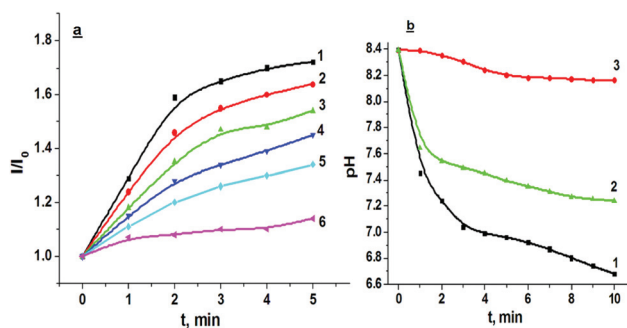


Fig. 7 (a)  $I/I_0$  versus time measured in the cluster complex solution (0.0075 mM),  $2 \times 10^{-8}$  M AChE, 0.4 mM ACh, 1 mM NaCl and no PyrBr (1) and in the presence of various PyrBr concentrations: 0.02 mM (2), 0.04 mM (3), 0.06 mM (4), 0.08 mM (5), 0.1 mM (6). (b) pH versus time measured for the same solution without inhibitor (1) and in the presence of 0.02 mM PyrBr (2) and 0.1 mM PyrBr (3).



concentrations. Results indicate the effect of inhibitor concentration on  $I/I_0$ . Analysis of  $I/I_0$  versus time (Fig. 7) shows slower release of acetic acid during the time course of AChE inhibition by PyrBr. Moreover, the greater the concentration of PyrBr the more the enzyme inhibited.

Good correlation between  $I/I_0$  and pH values measured at various times of the inhibition process under first order conditions,  $[E] \ll [\text{PyrBr}]$ , confirms that decrease in proton release is the cause for the observed difference in the cluster-centered luminescence response in the presence of a progressive inhibitor. The profiles of  $I/I_0$  versus time at various PyrBr concentrations (Fig. 7) are linear within two minutes. Corresponding slopes of linear dependencies decrease with increase in PyrBr concentration. This reflects PyrBr-induced inhibition of AChE. The inhibition is greater as PyrBr concentration is increased. The work of Forsberg<sup>55</sup> is worth noting for reporting the dissociation constant  $K_d$  of the reversible EI complex, the carbamylation constant  $k_2$  (4) and the bimolecular rate constant  $k_2/K_d$  for inhibition of AChE by PyrBr. Accurate determination of these constants is out of the scope of the present work and requires additional kinetic measurements, *i.e.*, inhibition by PyrBr in the presence of ACh at different concentrations.

The obtained results point to adequate sensing of both activity and inhibition of AChE through the luminescence response of the hexarhenium cluster complex. To the best of our knowledge, the present work is the first report about the applicability of cluster-centered luminescence in sensing enzymatic activity.

## Conclusions

The present work describes a new method for monitoring AChE-catalyzed hydrolysis of ACh through steady state luminescence of a hexarhenium cluster complex  $[\{\text{Re}_6\text{S}_8\}(\text{OH})_6]^{4-}$ . The method is based on sensitization of cluster-centered luminescence intensity by acetic acid. The protonation of hydroxyl groups without any changes in the cluster core results in significant enhancement of luminescence and excludes any rhenium-induced inhibiting effect due to the binding of rhenium cations to enzyme anionic centers. Results show a linear response of the cluster-centered luminescence to acetic acid, although the response is disturbed by background effects. Thus, specific conditions for adequate detection of acetic acid produced by AChE-catalyzed hydrolysis of ACh are highlighted.

Luminescence measurements were monitored within ten minutes of AChE-catalyzed hydrolysis of ACh. The monitored luminescence detects the release of acetic acid, although measurements are affected by proton-induced inhibition of AChE. However, the luminescence intensity measured within the first two minutes of hydrolysis provides adequate sensing of ACh enzymatic hydrolysis. The measured intensity as a function of substrate concentration fits the kinetic mechanisms of AChE- and BuChE-catalyzed hydrolysis of ACh. The applicability of the cluster-centered luminescence in monitoring

pyridostigmine-induced inhibition of AChE provides evidence that cluster-centered luminescence is a facile technique for fast and sensitive detection of any inhibitor of cholinesterases.

## Acknowledgements

We thank RSF (grant no 14-50-00014) for financial support. M. A. Shestopalov acknowledges the grant of the President of the Russian Federation (grant number MK 4054.2015.3) for financial support.

## Notes and references

- 1 E. G. Moore, A. P. S. Samuel and K. N. Raymond, *Acc. Chem. Res.*, 2009, **42**, 542–552.
- 2 R. N. Ghosh, P. A. Askeland, S. Kramer and R. Loloee, *Appl. Phys. Lett.*, 2011, **98**, 1103–1106.
- 3 S. Comby, E. M. Surender, O. Kotova, L. K. Truman, J. K. Molloy and T. Gunnlaugsson, *Inorg. Chem.*, 2014, **53**, 1867–1879.
- 4 A. R. Mukhametshina, A. R. Mustafina, N. A. Davydov, S. V. Fedorenko, I. R. Nizameev, M. K. Kadirov, V. V. Gorbachuk and A. I. Konovalov, *Langmuir*, 2015, **31**, 611–619.
- 5 S.-B. Yu and A. D. Watson, *Chem. Rev.*, 1999, **99**, 2353–2377.
- 6 M. Kubeil, H. Stephan, H.-J. Pietzsch, G. Geipel, D. Appelhans, B. Voit, J. Hoffmann, B. Brutschy, Y. V. Mironov, K. A. Brylev and V. E. Fedorov, *Chem. – Asian J.*, 2010, **5**, 2507–2514.
- 7 S.-J. Choi, K. A. Brylev, J.-Z. Xu, Y. V. Mironov, V. E. Fedorov, Y. S. Sohn, S.-J. Kim and J.-H. Choy, *J. Inorg. Biochem.*, 2008, **102**, 1991–1996.
- 8 C. Echeverria, A. Becerra, F. Nunez-Villena, A. Munoz-Castro, J. Stehberg, Z. Zheng, R. Arratia-Perez, F. Simon and R. Ramirez-Tagle, *New J. Chem.*, 2012, **36**, 927–932.
- 9 O. A. Efremova, M. A. Shestopalov, N. A. Chirtsova, A. I. Smolentsev, Y. V. Mironov, N. Kitamura, K. A. Brylev and A. J. Sutherland, *Dalton Trans.*, 2014, **43**, 6021–6025.
- 10 M. A. Shestopalov, K. E. Zubareva, O. P. Khripko, Y. I. Khripko, A. O. Solovieva, N. V. Kuratieva, Y. V. Mironov, N. Kitamura, V. E. Fedorov and K. A. Brylev, *Inorg. Chem.*, 2014, **53**, 9006–9013.
- 11 A. A. Krasilnikova, M. A. Shestopalov, K. A. Brylev, I. A. Kirilova, O. P. Khripko, K. E. Zubareva, Y. I. Khripko, V. T. Podorognaya, L. V. Shestopalova, V. E. Fedorov and Y. V. Mironov, *J. Inorg. Biochem.*, 2015, **144**, 13–17.
- 12 S. Cordier, Y. Molard, K. A. Brylev, Y. V. Mironov, F. Grasset, B. Fabre and N. G. Naumov, *J. Cluster Sci.*, 2015, **26**, 53–81.
- 13 S. Cordier, F. Grasset, Y. Molard, M. Amela-Cortes, R. Boukherroub, S. Ravaine, M. Mortier, N. Ohashi, N. Saito and H. Haneda, *J. Inorg. Organomet. Polym.*, 2015, **25**, 189–204.



- 14 J. Elistratova, M. Mikhailov, V. Burilov, V. Babaev, I. Rizvanov, A. Mustafina, P. Abramov, M. Sokolov, A. Konovalov and V. Fedin, *RSC Adv.*, 2014, **4**, 27922–27930.
- 15 K. A. Brylev, M. A. Shestopalov, O. P. Khripko, V. A. Trunova, V. V. Zvereva, C.-C. Wang, Y. V. Mironov and V. E. Fedorov, *Bull. Exp. Biol. Med.*, 2013, **155**, 741–744.
- 16 T. G. Gray, C. M. Rudzinski, E. E. Meyer, R. H. Holm and D. G. Nocera, *J. Am. Chem. Soc.*, 2003, **125**, 4755–4770.
- 17 K. A. Brylev, Y. V. Mironov, S. G. Kozlova, V. E. Fedorov, S.-J. Kim, H.-J. Pietzsch, H. Stephan, A. Ito, S. Ishizaka and N. Kitamura, *Inorg. Chem.*, 2009, **48**, 2309–2315.
- 18 K. A. Brylev, Y. V. Mironov, V. E. Fedorov, S.-J. Kim, H.-J. Pietzsch, H. Stephan, A. Ito and N. Kitamura, *Inorg. Chim. Acta*, 2010, **363**, 2686–2691.
- 19 A. Gandubert, K. A. Brylev, T. T. Nguyen, N. G. Naumov, N. Kitamura, Y. Molard, R. Gautier and S. Cordier, *Z. Anorg. Allg. Chem.*, 2013, **639**, 1756–1762.
- 20 K. Kirakci, P. Kubat, J. Langmaier, T. Polivka, M. Fuciman, K. Fejfarova and K. Lang, *Dalton Trans.*, 2013, **42**, 7224–7232.
- 21 H. Soreq and S. Seidman, *Nat. Rev. Neurosci.*, 2001, **2**, 294–302.
- 22 Y. Q. Miao, N. Y. He and J. J. Zhu, *Chem. Rev.*, 2010, **110**, 5216–5234.
- 23 O. Holas, K. Musilek, M. Pohanka and K. Kuca, *Expert Opin. Drug Discovery*, 2012, **7**, 1207–1223.
- 24 M. Pohanka, *Anal. Lett.*, 2013, **46**, 1849–1868.
- 25 J. Z. Zhang, A. M. Luo, P. Liu, S. P. Wei, G. M. Wang and S. Q. Wei, *Anal. Sci.*, 2009, **25**, 511–515.
- 26 M. Hoskovicova and Z. Kobliha, in *Environmental Biosensors*, ed. V. Somerset, InTech, Rijeka, Croatia, 2011, pp 65–94.
- 27 A. Watson, D. Opresko, R. A. Young, V. Hauschild, J. King, K. Bakshi and R. C. Gupta, in *Handbook of Toxicology of Chemical Warfare Agents*, ed. R. C. Gupta, Academic Press, Boston, 2015, pp. 87–109.
- 28 M. L. Bolognesi, V. Andrisano, M. Bartolini, R. Banzi and C. Melchiorre, *J. Med. Chem.*, 2005, **48**, 24–27.
- 29 T. Sauvaitre, M. Barlier, D. Herlem, N. Gresh, A. Chiaroni, D. Guenard and C. Guillou, *J. Med. Chem.*, 2007, **50**, 5311–5323.
- 30 S. Darvesh, K. V. Darvesh, R. S. McDonald, D. Mataija, R. Walsh, S. Mothana, O. Lockridge and E. Martin, *J. Med. Chem.*, 2008, **51**, 4200–4212.
- 31 R. Makkar, P. Singh, C. C. Danta, V. Kakkar, I. P. Kaur and P. Piplani, *Curr. Drug Ther.*, 2014, **9**, 111–123.
- 32 T. L. Rosenberry, *Proc. Natl. Acad. Sci. U. S. A.*, 1975, **72**, 3834–3838.
- 33 A. R. Main, *Pharmacol. Ther.*, 1979, **6**, 579–628.
- 34 G. L. Ellman, K. D. Courtney, V. Andres jr. and R. M. Featherstone, *Biochem. Pharmacol.*, 1961, **7**, 88–95.
- 35 R. S. Naik, W. Y. Liu and A. Saxena, *J. Appl. Toxicol.*, 2013, **33**, 290–300.
- 36 J. J. Chance, E. J. Norris and M. H. Kroll, *Clin. Chem.*, 2000, **46**, 1331–1337.
- 37 M. Pohanka and V. Vlcek, *Interdiscip. Toxicol.*, 2014, **7**, 215–218.
- 38 M. Wang, X. G. Gu, G. X. Zhang, D. Q. Zhang and D. B. Zhu, *Anal. Chem.*, 2009, **81**, 4444–4449.
- 39 D. L. Liao, J. Chen, H. P. Zhou, Y. Wang, Y. X. Li and C. Yu, *Anal. Chem.*, 2013, **85**, 2667–2672.
- 40 S. Z. Liao, W. T. Han, H. Z. Ding, D. X. Xie, H. Tan, S. Y. Yang, Z. Y. Wu, G. L. Shen and R. Q. Yu, *Anal. Chem.*, 2013, **85**, 4968–4973.
- 41 Y. D. Zhang, Y. A. Cai, Z. L. Qi, L. Lu and Y. X. Qian, *Anal. Chem.*, 2013, **85**, 8455–8461.
- 42 Y. H. Yi, G. B. Zhu, C. Liu, Y. Huang, Y. Y. Zhang, H. T. Li, J. N. Zhao and S. Z. Yao, *Anal. Chem.*, 2013, **85**, 11464–11470.
- 43 A. R. Mukhametshina, S. V. Fedorenko, I. V. Zueva, K. A. Petrov, P. Masson, I. R. Nizameev, A. R. Mustafina and O. G. Sinyashin, *Biosens. Bioelectron.*, 2016, **77**, 871–878.
- 44 G. Tomlinson, B. Mutus, I. McLennan and M. J. Mooibroek, *Biochim. Biophys. Acta*, 1982, **703**, 142–148.
- 45 J. K. Marquis, *Comp. Biochem. Phys. C*, 1984, **78**, 335–338.
- 46 S. Mukhopadhyay, S. Mukhopadhyay, D. K. Bhattacharyya and G. C. Chatterjee, *J. Biosci.*, 1988, **13**, 123–128.
- 47 K. A. Brylev, Y. V. Mironov, S. S. Yarovoi, N. G. Naumov, V. E. Fedorov, S.-J. Kim, N. Kitamura, Y. Kuwahara, K. Yamada, S. Ishizaka and Y. Sasaki, *Inorg. Chem.*, 2007, **46**, 7414–7422.
- 48 P. Masson, L. M. Schopfer, C. F. Bartels, M. T. Froment, F. Ribes, F. Nachon and O. Lockridge, *Biochim. Biophys. Acta, Protein Struct. Mol. Enzymol.*, 2002, **1594**, 313–324.
- 49 P. Masson, *Biochemistry*, 2012, **77**, 1147–1161.
- 50 H. Leader, A. D. Wolfe, P. K. Chiang and R. K. Gordon, *J. Med. Chem.*, 2002, **45**, 902–910.
- 51 A. Fischer, M. Wolman, M. Granato, M. Parsons, A. S. McCallion, J. Proescher and E. English, *Neurotoxicol. Teratol.*, 2015, **50**, 1–10.
- 52 O. Lockridge, L. M. Schopfer, G. Winger and J. H. Woods, *J. Med. Chem. Biol. Radiol. Def.*, 2005, **3**, 5095–5115.
- 53 S. S. Yarovoi, Y. V. Mironov, D. Y. Naumov, Y. V. Gatilov, S. G. Kozlova, S.-J. Kim and V. E. Fedorov, *Eur. J. Inorg. Chem.*, 2005, 3945–3949.
- 54 V. Marcel, L. G. Palacios, C. Pertuy, P. Masson and D. Fournier, *Biochem. J.*, 1998, **329**, 329–334.
- 55 Å. Forsberg and G. Puu, *Eur. J. Biochem.*, 1984, **140**, 153–156.

